

Analysis of Nugget Formation During Resistance Spot Welding on Dissimilar Metal Sheets of Aluminum and Magnesium Alloys

YI LUO and JINGLONG LI

The nugget formation of resistance spot welding (RSW) on dissimilar material sheets of aluminum and magnesium alloys was studied, and the element distribution, microstructure, and microhardness distribution near the joint interface were analyzed. It was found that the staggered high regions at the contact interface of aluminum and magnesium alloy sheets, where the dissimilar metal melted together, tended to be the preferred nucleation regions of nugget. The main technical problem of RSW on dissimilar metal sheets of aluminum and magnesium alloys was the brittle-hard $Al_{12}Mg_{17}$ intermetallic compounds distributed in the nugget, with hardness much higher than either side of the base materials. Microcracks tended to generate at the interface of the nugget and base materials, which affected weld quality and strength.

DOI: 10.1007/s11661-014-2463-2

© The Minerals, Metals & Materials Society and ASM International 2014

I. INTRODUCTION

IN the automotive industry, lightweight automobiles are in strong demand because of the related fuel consumption reduction and natural resource savings.^[1,2] Aluminum and magnesium alloys belong to the structural materials of light alloy. Owing to their low density and significant mechanical properties, aluminum and magnesium alloys were adopted and are expected to be extensively used to replace steel as the primary structural material in automobiles.^[3] Resistance spot welding (RSW) is a largely used and important welding process in the automotive industry; RSW has the capacity to assemble thin sheets, such as austenitic stainless steel, zinc-coated steel, titanium alloy, aluminum alloy, and magnesium alloy.^[4–8]

Owing to the fact that the consumption of light alloy materials in the automobile industry has been gradually increasing, the RSW of different alloys is seeing increased demand. Researchers have conducted many studies regarding the RSW of dissimilar metal materials. Galvanized steel and stainless steel sheet are widely used in the manufacture of automobiles. Marashi and others used RSW to join austenitic stainless steel and galvanized low carbon steel and studied the relationship between the failure mode and weld fusion zone characteristics, including the nugget size and microstructure. As the physical properties of both materials were close, a high welding reliability of weld joints was obtained.^[9] Naffakh *et al.* conducted a study to characterize the welding of AISI 310 austenitic stainless steel to the

INCONEL 657 nickel-chromium superalloy, especially the fracture mode of the joint and its characteristics.^[10]

A large number of studies also revealed that the quality of weld joints had a close relationship to the formation process of RSW nugget. Therefore, some researchers paid attention to the process and mechanism of RSW nugget formation. Electrical contact resistance is of critical importance in resistance welding. Feng and others studied the formation characteristics of nugget during RSW on AZ31B magnesium alloy using the numerical simulation method. The results showed that the contact resistance at the interface has a significant effect on nugget formation. The welding process parameters, including welding time and welding current level, are similar to those in Al alloy welding.^[11] The contact resistance was experimentally investigated for the welding of mild steel, stainless steel, and aluminum to themselves in the experiments of Song and others. The results showed the influence of interface normal pressure, temperature, and base metal on contact resistance.^[12] The measurements concerning sheet materials with coatings, electrode-sheet and sheet-sheet interfaces, also proved that the contact resistance under temperature and pressure has similar results.^[13] In addition, some researchers also used numerical simulation and experimental methods to study the influence of the surface contact state upon the welding quality and formation characteristics of RSW nugget, which proved that a successful application of RSW requires careful consideration of the surface condition of sheet.^[14–16]

However, the welding quality does not only depend on the formation of RSW nugget, but also has a close relationship with the microstructure of nugget interface and properties for the RSW of dissimilar material sheets of aluminum and magnesium alloys. This study mainly focuses on the RSW of dissimilar material sheets of magnesium and aluminum alloys on the basis of the research of our predecessors, including studies on the formation process of RSW nugget and the microstructure and properties around the joint interface.

YI LUO, Professor, is with the School of Material Science and Engineering, Chongqing University of Technology, Chongqing 400054, P.R. China. Contact e-mail: luoyi@cqut.edu.cn JINGLONG LI, Professor, is with the State Key Laboratory of Solidification Processing, Northwestern Polytechnical University, Xi'an 710072, Shaanxi, P.R. China.

Manuscript submitted April 5, 2013.
Article published online July 19, 2014

Table I. Chemical Compositions of AZ31B Magnesium Alloy and 2024 Aluminum Alloy

Material	Element (wt pct)										
	Mg	Al	Zn	Mn	Si	Cu	Fe	P	Pb	Be	Cr
AZ31B	96.2467	2.8150	0.6395	0.2835	0.0094	0.0004	0.0025	0.0013	0.0008	0.0009	—
2024	1.5	92.15	0.25	0.65	0.50	4.35	0.50	—	—	—	0.10

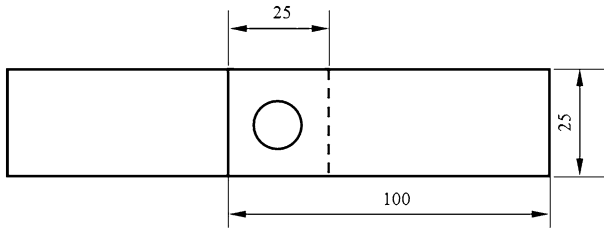


Fig. 1—Specimen dimensions (mm).

Table II. Welding Parameters of RSW

Weld Number	Thickness, H (mm)	Welding Current, I (A)	Current Duration, t (s)	Electrode Force, P (MPa)
1	2.0 + 2.0	29,000	0.12	0.1
2	2.0 + 2.0	29,000	0.16	0.1

II. MATERIALS AND EXPERIMENTS

The materials used in the experiments are 2024 aluminum alloy with 1-mm thickness and AZ31B magnesium alloy with 2-mm thickness; the chemical compositions are shown in Table I. The dimensions of the samples are 25 mm \times 100 mm. Two specimens are welded and overlap by 25-mm lengths, as shown in Figure 1. A RSW machine having 100-kVA capacity is used in the experiment, the material of the electrodes is pure copper, and the electrode diameter is 8 mm.

Surface chemical cleaning is used to process specimens before welding, and the welding parameters are shown in Table II. The etching agent used in the experiment for metallography is a mixture composed of 2 g trinitrophenol, 50 mL alcohol, and 20 mL acetic acid. The microhardness of the spot weld is tested by 100 g loaded force and 15-second loading time. The interval distance of hardness points is 0.1 mm.

III. RESULTS AND DISCUSSION

A. Formation of RSW Nugget at the Interface

A larger amount of contact resistance heat at the contact interface, higher than the resistance heat in materials at the beginning period of RSW nugget formation, will generate the welding current passing

through the pieces of metal due to the contact resistance at the pressed interface of the specimen. Therefore, the formation of RSW nugget will preferentially form at the contact interface. Figure 2 is the formation evolution of RSW nugget at the joint interface under different welding energy effects. Because of the relatively short current duration for weld 1, the contact resistance heat generated is conducted and lost so quickly that it cannot induce the generation of nugget effectively. The joint interface makes a clear distinction between the two materials. However, there is enough time for the welding current to generate a large amount of resistance heat at the contact interface for weld 2. The region around the contact interface is melted; further, the melted region gradually extends to form nugget, so as to cause the welding effect.

It can be further found that there is a certain amount of plastic deformation generated at the contact interface with the effects of resistance heat and electrode pressure when the welding energy is low, but the joint interfaces show basically no nugget formation and are still in a state of separation (Figure 3(a)). However, the base materials on the side of the magnesium alloy are softened and melted prior to aluminum alloy as the weld energy increases and the plastically deforming region expands, and the aluminum alloy intrudes into the magnesium alloy. Therefore, the weld line becomes macroscopically displaced, developing a convoluted wavelike appearance (Figure 3(b)). As the resistance heat continues to cause the contact interface to produce further melting, these protrusion regions of dissimilar material (arrows 2 and 3 in Figure 2(b)) are conducive to the mixing of dissimilar materials at the joint interface (arrow 4 in Figure 2(b)) and the further formation of RSW nugget, then preferentially forms nugget. At last, nugget with a certain macroscale is formed, as arrow 1 in Figure 2(b) shows.

B. Element Distribution Around the Joint Interface

The element distributions around the joint interface are shown in Figure 4. It can be seen that there is no remarkable nugget formation along the boundaries of aluminum and magnesium alloys at the joint interface, and almost no diffusion of Mg or Al has taken place around the interface (Figure 4(a)). So, the nugget has not formed at the joint interface. Correspondingly, there is a significant diffusion zone of aluminum and magnesium elements at the joint interface that is the

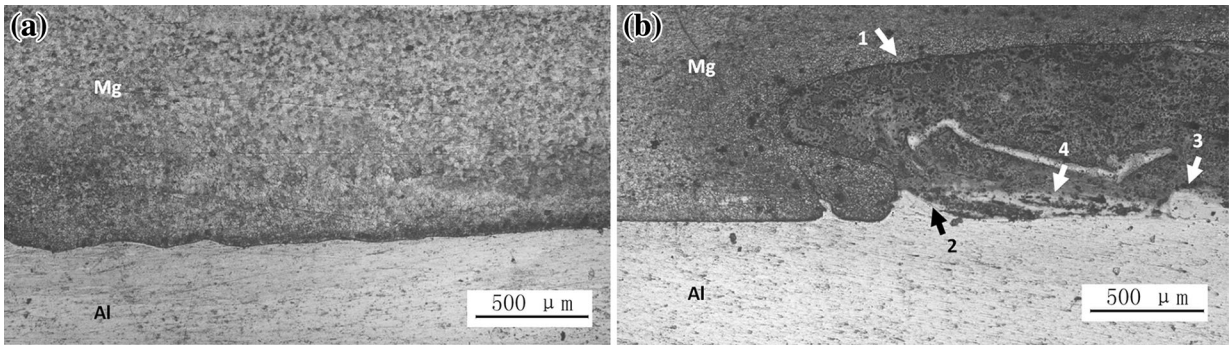


Fig. 2—Formation of RSW nugget appearance at the joint interface: (a) weld 1, without any nugget formed at the joint interface—29,000 A, 0.12 s, 0.1 MPa; and (b) weld 2, with nugget formed at the joint interface—29,000 A, 0.16 s, 0.1 MPa.

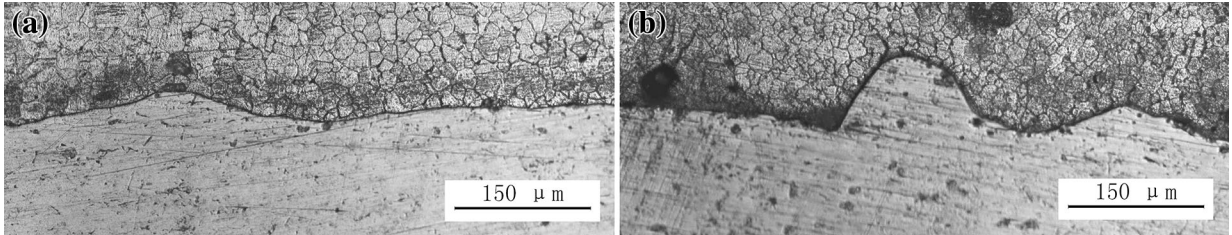


Fig. 3—Initial formation of RSW nugget at the joint interface with different welding parameters: (a) weld 1—29,000 A, 0.12 s, 0.1 MPa; and (b) weld 2—29,000 A, 16 s, 0.1 MPa.

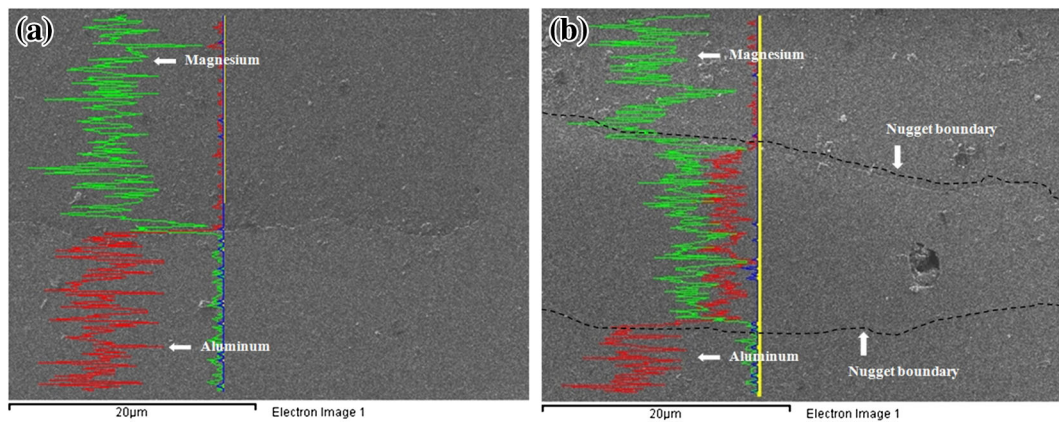


Fig. 4—Energy spectrum analysis of alloy elements at (a) the joint interface with no nugget and (b) the joint interface with formation of RSW nugget.

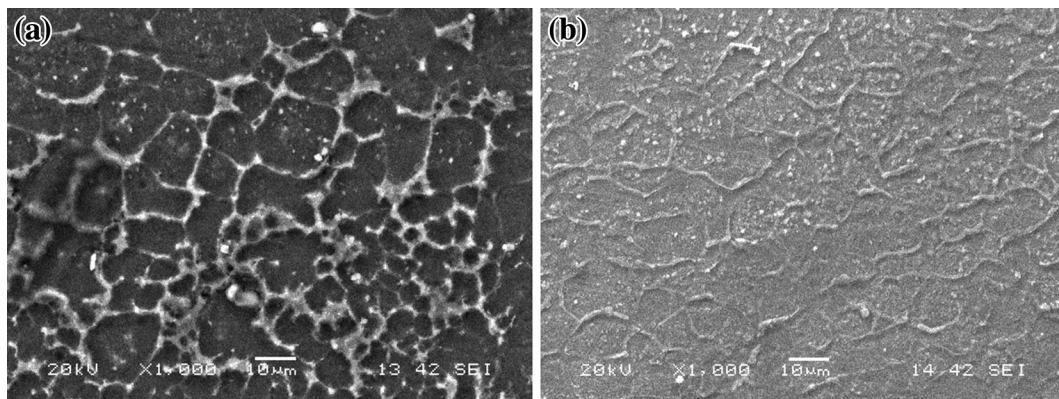


Fig. 5—Microstructure on the side of the (a) magnesium alloy base material and (b) aluminum alloy base material around the nugget.

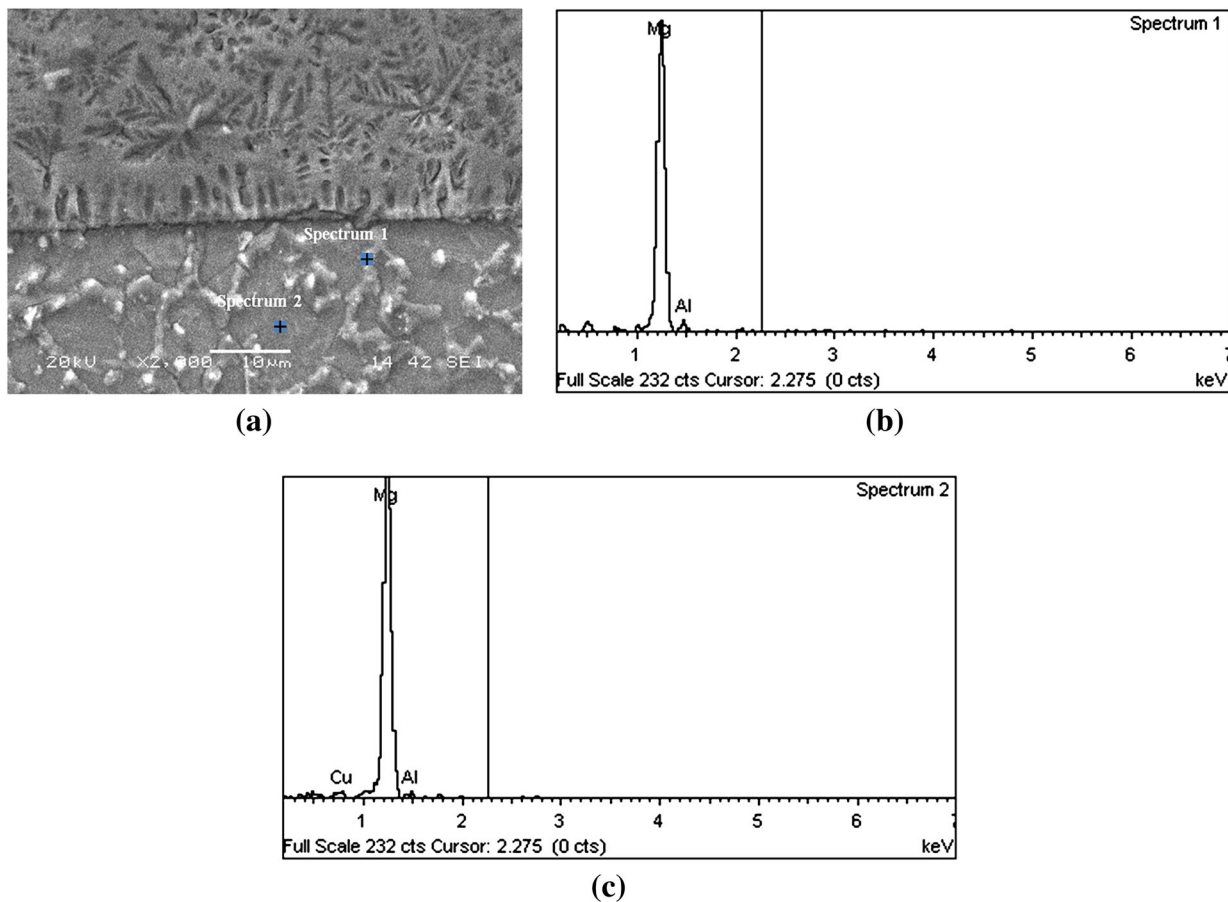


Fig. 6—Microstructure around the joint interface and energy spectrum analysis of composition: (a) microstructure, (b) EDS of composition at spectrum 1, and (c) EDS of composition at spectrum 2 on the side of the magnesium alloy.

Table III. Compositional Analysis of the Phases on the Side of the Base Metal of AZ31B

Spectrum	Mg (wt pct)	Al (wt pct)	Cu (wt pct)
1	90.37	9.63	—
2	94.07	5.01	0.91

primary nugget in Figure 4(b). The primary nugget that is Mg-Al alloy will be further developed into a larger nugget with continuing or stronger resistance heat effects.

C. Microstructure Around the Joint Interface

Figure 5 shows the microstructure of the base metals of magnesium and aluminum alloys around the nugget, which appears to be partially melted. Figure 5(a) is the

microstructure of the magnesium alloy base metal affected by the welding thermal effect, which mainly includes the isometric grains consisting of α -Mg and β precipitates. Figure 5(b) is the microstructure of aluminum alloy base metal affected by the welding thermal effect, which mainly includes the eutectic consisting of α -Al and MgCuAl₂.

Figure 6 shows the microstructure on either side of the joint interface. The upper region is nugget and the lower region is the base metal of magnesium alloy. Both sides have significant differences in microstructure (Figure 6(a)), and the nugget remains clearly visible as its dendrites are set off by the equiaxed grains in the base metal. Through energy spectrum analysis (EDS) of the distribution of alloying elements on the side of the magnesium alloy base material (Figures 6(b) and (c) and Table III), it can be found that the solid solution Mg-Al alloys mainly distribute on the side of the magnesium base metal near the joint interface. Figure 7 shows the

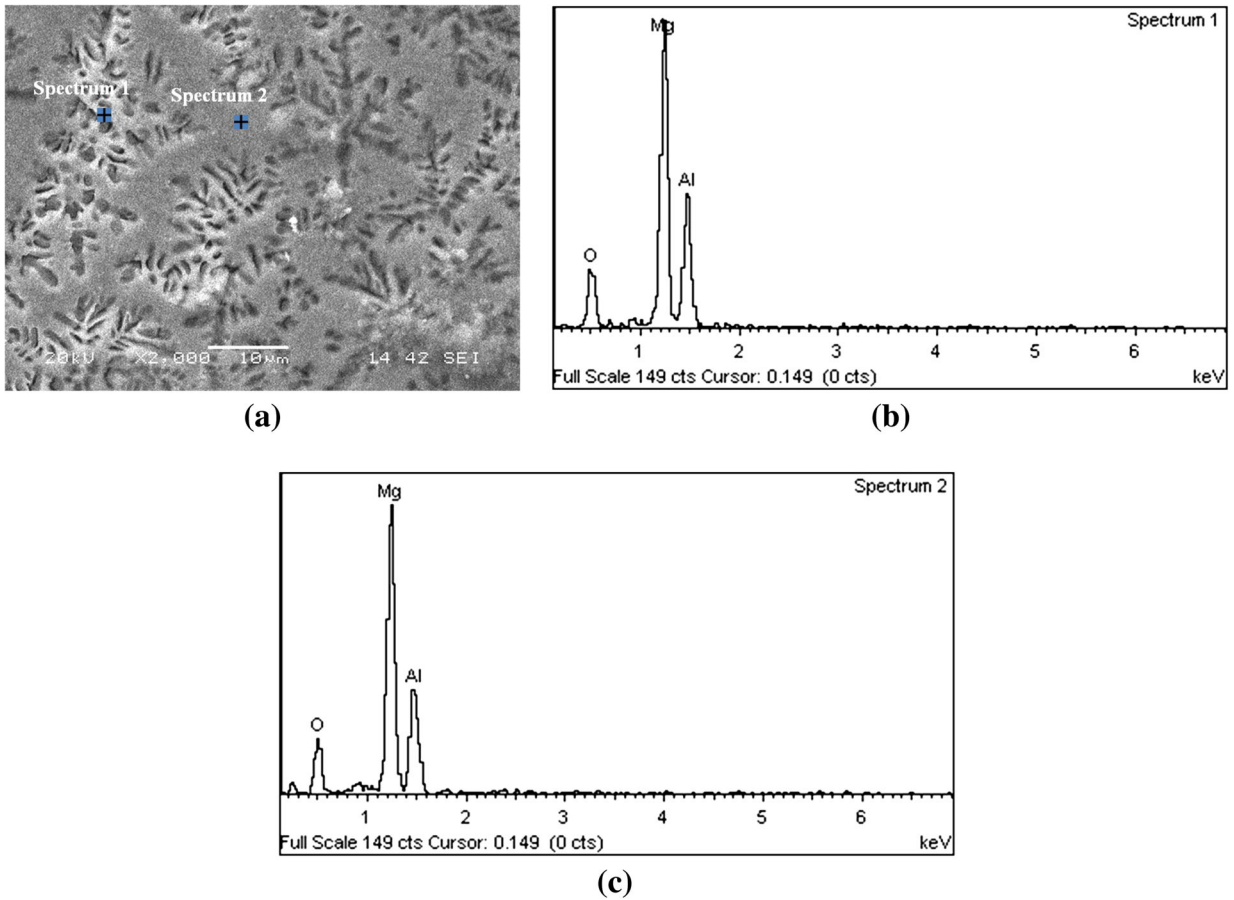


Fig. 7—Microstructure in the nugget and energy spectrum analysis of composition: (a) microstructure in the nugget and (b) and (c) EDS of composition to the phases of the nugget at spectra 1 and 2.

Table IV. Phases in Nugget

Spectrum	Mg (wt pct)	Al (wt pct)	O (wt pct)
1	40.73	30.05	29.22
2	42.57	28.18	29.25

microstructure on the side of nugget near the joint interface. It can be found that there are a large number of isometric dendrites distributed in nugget (Figure 7(a)). From the energy spectrum analysis of dendrite and grain boundary elements in nugget (Figures 7(b) and (c) and Table IV), it can be found that the mass percentages of the Mg element at spectra 1 and 2, respectively, are 55.2 and 60.2 wt Pct. According to the binary alloy phase diagram of Mg-Al (Figure 8), it can be determined that the phase composition of nugget is mainly $Al_{12}Mg_{17}$ intermetallic compound, which is brittle and hard.

D. Microhardness Around the Joint Interface

Figure 9 presents the microhardness distribution near the joint interface. For the joint interfaces with no RSW nugget, microhardness distributions on both sides have significant differences. There is almost no transition area between the aluminum and magnesium alloys (Figure 9(a)), which also means that nugget is not formed at the joint interface. For the joint interface with the formation of RSW nugget (Figure 9(b)), it can be found that the microhardness in nugget is well above both sides of the base metals; that is, the nugget phase composed of $Al_{12}Mg_{17}$ intermetallic compounds has higher hardness. High hardness of $Al_{12}Mg_{17}$ intermetallic compounds in nugget is the main problem with RSW on dissimilar materials of aluminum and magnesium alloys. Due to the high hardness and low plasticity of $Al_{12}Mg_{17}$ intermetallic compounds in nugget, the mechanical properties of nugget are vastly different from either side of aluminum or magnesium alloy, which makes it extremely easy to induce microcracks at

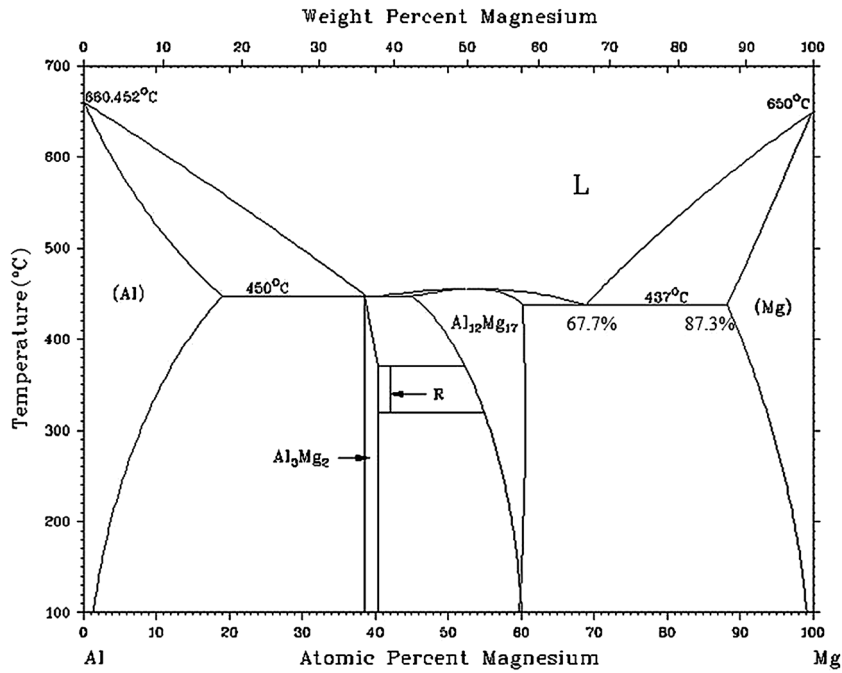


Fig. 8—Binary alloy phase diagram of Mg-Al.^[17]

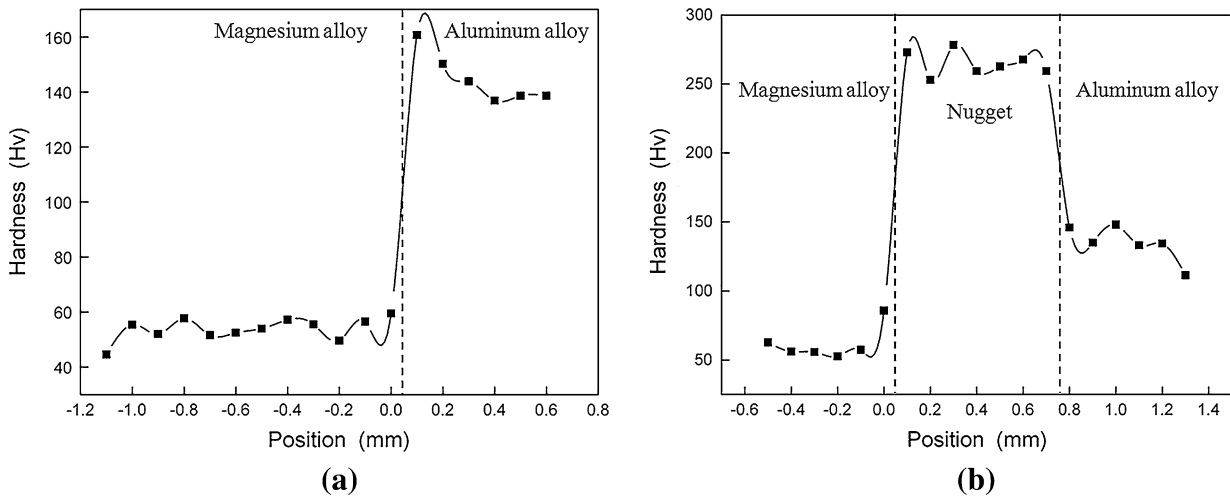


Fig. 9—Microhardness distribution around the joint interface (a) with no nugget and (b) with formation of RSW nugget.

the transition interface. The arrows in Figure 10 point out the microcracks at the interface of the nugget and base metal of the magnesium alloy, in which the upper region is nugget and the lower region is the magnesium alloy base material. Due to the existence of such

microcracks and brittle and hard $\text{Al}_{12}\text{Mg}_{17}$ in nugget, fracture failure of weld can occur under low load conditions. These problems have brought about tremendous difficulties for the RSW of dissimilar materials of aluminum and magnesium alloys, and other

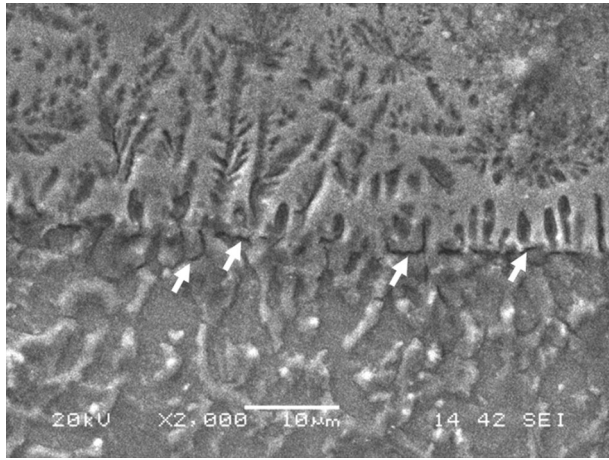


Fig. 10—Microcracks at the joint interface.

technologies are needed to achieve the RSW of these two materials.

IV. CONCLUSIONS

1. The protrusion regions of dissimilar material at the contact interface preferentially form nugget during RSW on the aluminum and magnesium alloys. The existence of these regions also is conducive to the mixing of dissimilar material at the joint interface and further formation of RSW nugget.
2. RSW nugget of aluminum and magnesium alloys is distributed with a large number of brittle and hard $Al_{12}Mg_{17}$ intermetallic compounds, whose hardness is much higher than either side of the base metal of aluminum or magnesium alloy. This difference of hardness makes it extremely easy to induce microcracks at the transition interface and affects welding quality and weld strength.

ACKNOWLEDGMENTS

This work was supported by Scientific and Technological Research Program of Chongqing Municipal Education Commission of China (Grant No. KJ1400930), the fund of the State Key Laboratory of Solidification Processing in NWPU (Grant No. SKLSP201204), and the Major Project of Outstanding Achievements Conversion of Chongqing Colleges (Grant No. KJZH11215).

REFERENCES

1. D. Bakavos and P.B. Prangnell: *Mater. Sci. Eng. A*, 2010, vol. 527, pp. 6320–34.
2. D.Q. Sun, B. Lang, D.X. Sun, and J.B. Li: *Mater. Sci. Eng. A*, 2007, vols. 460–461, pp. 494–98.
3. R.F. Qiu, S. Satonaka, and C. Lwamoto: *Sci. Technol. Weld. Join.*, 2009, vol. 14, pp. 691–97.
4. N. Kahraman: *Mater. Des.*, 2007, vol. 28, pp. 420–27.
5. D. Ozyurek: *Mater. Des.*, 2008, vol. 29, pp. 597–603.
6. Y.R. Wang, J.C. Feng, and Z.D. Zhang: *Sci. Technol. Weld. Join.*, 2006, vol. 11, pp. 555–60.
7. Y.R. Wang, Z.H. Mo, J.C. Feng, and Z.D. Zhang: *Sci. Technol. Weld. Join.*, 2007, vol. 12, pp. 641–46.
8. Y. Luo, J.H. Liu, H.B. Xu, C.Z. Xiong, and L. Liu: *Mater. Des.*, 2009, vol. 30, pp. 2547–55.
9. P. Marashi, M. Pouranvari, S. Amirabdollahian, A. Abedi, and M. Goodarzi: *Mater. Sci. Eng. A*, 2008, vol. 480, pp. 175–80.
10. H. Naffakh, M. Shamanian, and F. Ashrafizadeh: *J. Mater. Process. Technol.*, 2009, vol. 209, pp. 3628–39.
11. J.C. Feng, Y.R. Wang, and Z.D. Zhang: *Sci. Technol. Weld. Join.*, 2006, vol. 11, pp. 154–62.
12. Q.F. Song, W.Q. Zhang, and N. Bay: *Weld. J.*, 2005, vol. 84, pp. 73s–6s.
13. P. Rogeon, P. Carre, J. Costa, G. Sabilia, and G. Saindrenan: *J. Mater. Process. Technol.*, 2008, vol. 195, pp. 117–24.
14. G. Le Meur, B. Bourouga, and T. Dupuy: *Sci. Technol. Weld. J.*, 2003, vol. 8, pp. 415–22.
15. E. Feulvarch, V. Robin, and J.M. Bergheau: *J. Mater. Process. Technol.*, 2004, vols. 153–154, pp. 436–41.
16. L. Han, M. Thornton, D. Boomer, and M. Shergold: *J. Mater. Process. Technol.*, 2010, vol. 210, pp. 1076–82.
17. S.F. Su, J.C. Huang, H.K. Lin, and N.J. Ho: *Metall. Mater. Trans. A*, 2002, vol. 33A, pp. 1461–73.